

Adaptive Dynamic Surface Control of Chaotic Micro-Electro-Mechanical System with Unknown System Parameters and Dead-Zone Input

Shaohua Luo*, Suqun Cao**, Zhong Chen*** and K. Sujatha****

*The Jiangsu Key Laboratory of Advanced Manufacturing Technology, Huaiyin Institute of Technology, Huai'an 223003, China; School of Automation, Chongqing University, Chongqing 400044, China
hua66com@163.com

** The affiliated Huai'an Hospital of Xuzhou Medical College, Huai'an 223003, China ; School of Computer Science and Engineering, Southeast University, Nanjing 211189, China; Faculty of Mechanical and Material Engineering, Huaiyin Institute of Technology, Huai'an 223003, China
caosuqun@126.com

***The Jiangsu Key Laboratory of Advanced Manufacturing Technology, Huaiyin Institute of Technology, Huai'an 223003, China
chenzhong2006@126.com

****EEE Department, Center for Electronics, Automation and Industrial Research (CEAIR), Dr. M.G.R. Educational and Research Institute, Maduravoyal, Chennai - 600095, Tamil Nadu, India
drksujatha23@gmail.com

Abstract: This paper focuses on chaos control of the micro-electro-mechanical system with unknown system parameters and dead-zone input existing in the engineering application. The phase diagrams, corresponding time histories and bifurcation diagram are employed to reveal the chaotic dynamics performance of the micro-electro-mechanical system. For eliminating chaos and vibration, an adaptive neural-network-based dynamic surface control is proposed to convert the chaos motion into regular motion without imposing any condition on parameters of system model and the boundedness of control gain. Meanwhile, to achieve high accuracy and quick response, a neural network is employed to approximate unknown nonlinear item of model and an adaptive law is designed to estimate unknown control gain in the framework of dynamic surface control. Finally, some simulations are executed and corresponding results show effectiveness and robustness of the proposed scheme.

Keywords: Micro-electro-mechanical system; Adaptive dynamic surface control; Chaos control; Neural network; Dead-zone input.

Introduction

The research aimed at micro-electro-mechanical system has garnered significant attention recently because of its advantages. A lot of researches have been carried out on the behaviors and modeling. Though some achievements about micro-electro-mechanical system have been made, there still exists some challenges associated with it¹⁻³. A key problem is how to effectively control chaotic behavior of micro-electro-mechanical system with unknown system parameters and dead-zone input. Chaos phenomenon with geometrical strangeness usually leads to deterioration of the system performance.

To suppress chaos in the motion process of micro-electro-mechanical system, various methods and analysis results have been reported recently^{4,5}. The OGY is a basic method for suppressing chaos behavior⁶. But it is difficult to choose a reasonable parameter in real practice. Chaos control using the time-delay feedback control method is introduced to the engineering applications⁷. But it is applied under strict restriction that the control objective must be the equilibrium. For suppressing the chaos motion, the robust fuzzy sliding mode controller is designed⁸. This approach uses fuzzy logic linguistic rules to generate a suitable chatter-free control signal for driving the error dynamic system and ensures the track error to converge asymptotically to zero. The drawback of this approach needs to obtain precision model in the process of design. However, the parameters of system and actuator dead-zone input are hard to do a high-precious measurement because parameters are influenced by temperature and material wear.

Sliding mode control (SMC) is recognized as a useful and effective approach, which deals with time varying properties, uncertainties and bounded external disturbances^{9,10}. However, the chattering associated with SMC is a serious impediment for engineering application. In view of this, a novel second-order fast terminal sliding mode control is proposed to suppress the random motion of the micro-electro-mechanical system with system uncertainty and external disturbance¹¹. The dynamic surface control (DSC) is proposed by introducing a first-order filtering of the synthetic input at each step of the backstepping,

so the differentiation items on the virtual function can be thoroughly eliminated¹². An adaptive dynamic surface control combined with SMC to compensate for friction and backlash nonlinearities in a motion system is designed, wherein the updated laws of the recurrent wavelet neural networks and friction estimation are derived to approximate and compensate for the backlash and friction nonlinearities¹³. However, the explicit consideration of input constraint within the framework of DSC have not received attention. Furthermore, the control gain which is usually unknown in real environment is supposed to a bounded constant in previous works. To solve it, the Nussbaum gain is adopted to deal with unknown sign on the problem of input uncertainty^{14, 15}. Then, the unknown gain can be effectively estimated in finite time. But the drawback is the complicated calculation procedures and time consuming.

Dead-zone input usually exists in the control input because of the actuator’s physical limitations^{16, 17}. This nonlinearity can cause oscillation and then deteriorate the micro-electro- mechanical system performance. An adaptive control method based on neural network is presented to control a direct current motor system with dead-zone characteristics, wherein neural networks are adopted to accomplish traditional identification¹⁸. Unfortunately, this research result is only limited to symmetric dead-zone input.

Many researchers have achieved considerable progress in chaos of the micro-electro-mechanical system, but chaos control remains to face new challenges. In this paper, an adaptive dynamic surface control combining with neural network is designed to apply on tracking control for the micro-electro-mechanical system with unknown system parameters and dead-zone input. First, the scheme is designed by Lyapunov stability theory, which can guarantee stabilization of the closed-loop error system. Second, in the recursive process of DSC, a neural network is employed to approximate unknown nonlinear item of math model which reduces the requirement about precise parameters. It not only improves tracking accuracy but also obtains a smooth control input without high-frequent chattering phenomena. Moreover, stability analysis is carried out so that the error converges to a small neighborhood of the origin. Finally, numerical simulation results show a satisfactory performance.

System description

System model

The schematic diagram of the micro-electro-mechanical system under the combined DC and AC actuation voltages is depicted in Fig.1. An external driving force on the resonator is implemented by using an electrical driving voltage that leads to electrostatic excitation between electrodes and resonator.

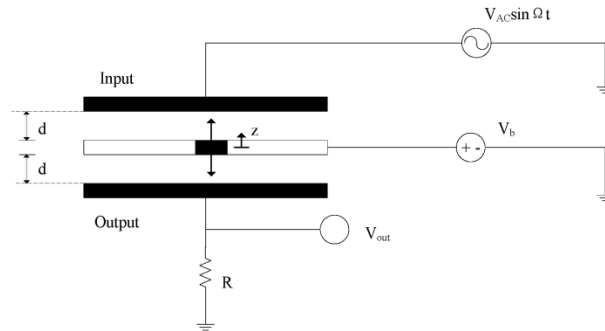


Fig 1.Schematic diagram of the micro-electro-mechanical system

For establishing dynamic model, it makes assumptions that the amplitude of the AC driving voltage is much lower than the bias voltage. Then, the math model of chaotic micro-electro- mechanical system can be defined as follow⁵.

$$\ddot{x} + \mu\dot{x} + \alpha x + \beta x^3 = \gamma \left(\frac{1}{(1-x)^2} - \frac{1}{(1+x)^2} \right) + \frac{A}{(1-x)^2} \sin(\omega\tau) \tag{1}$$

where the non-dimensional variables x and ω are defined as

$$x = \frac{z}{d}, \omega = \frac{\Omega}{\omega_0}, A = 2\gamma \frac{V_{AC}}{V_b}$$

where d is the initial width of the gap, z is the vertical displacement of the beam midpoint, Ω is the frequency of AC voltage, ω_0 is the natural frequency, V_{AC} is the AC amplitude, V_b is the bias voltage.

For simplicity, the following notations are employed:

$$x_1 = x, x_2 = \dot{x}, G(x) = \gamma \left(\frac{1}{(1-x)^2} - \frac{1}{(1+x)^2} \right) \quad (2)$$

Substituting the notations into (1) yields the following nominal form with non-symmetric dead-zone input.

$$\begin{cases} \dot{x}_1 = x_2 \\ \dot{x}_2 = -\mu x_2 - \alpha x_1 - \beta x_1^3 + G + \frac{A}{(1-x_1)^2} \sin(\omega\tau) + \Gamma(u) \end{cases} \quad (3)$$

The micro-electro-mechanical system has been studied for V_{AC} in $(0, 0.47)$ and constant values of $\alpha = 1$, $\beta = 12$, $\gamma = 0.338$, $\mu = 0.01$, $V_b = 3.8$ and $\omega = 0.5$. The phase diagrams and corresponding time histories are shown in Fig. 2 in given initial conditions like $(x_1, x_2) = (0, 0)$ and the fixed bias voltage. Beginning at the neighboring value of zero, the transient chaos and regular motion around the center points are shown in Fig. 2(a). Obviously, the more increase in AC voltage gives rise to longer transient and random vibration. As can be seen from the Fig. 2(c), after the transient chaotic response, regular motion can come into being in homoclinic orbit and the amplitude of harmonic oscillation is much larger comparing to the case in Fig. 2(a)-(b). Fig. 3 shows the bifurcation diagram. In the case, the qualitative behavior of the micro-electro-mechanical system is concluded against a varying voltage from 0 to 0.4. Along with increasement of AC voltage, regular motion appears around one of the center points.

Actuator dead-zone input

Actuator dead-zone input which is considered as a complex nonlinearity phenomenon occurs in the micro-electro-mechanical system. The phenomenon usually leads to oscillatory activity and deteriorates the system performance. Thus, it is necessary to eliminate it.

The non-symmetric dead-zone of actuator can be written as a combination of a line and a disturbance-like term¹⁹

$$\Gamma(u) = m(t)u + d_1(t) \quad (4)$$

$$\text{where } m(t) = \begin{cases} m_r, u \leq 0 \\ m_l, u > 0 \end{cases}, d_1(t) = \begin{cases} -m_r b_r, u \geq b_r \\ -m(t)u, -b_l < u < b_r \\ m_l b_l, u \leq -b_l \end{cases}, m_r \text{ and } m_l \text{ stand for the right and left slopes of the dead-zone}$$

characteristic, respectively, b_r and b_l denote the breakpoint of the actuator dead-zone input, respectively.

Chaos controller

In this section, an adaptive neural-network-based dynamic surface control method is used to stabilize the micro-electro-mechanical system with non-symmetric dead-zone input in a high amplitude oscillation state. The proposed scheme can easily accommodate change and has strong robustness in the face of dynamic uncertainties.

The boundary layer error is given in the first place as follow

$$y_2 = \alpha_{2f} - \alpha_2 \quad (5)$$

where α_{2f} is the output of the first-order filter, α_2 is the virtual control input.

Then, for any given x_{1d} , the dynamic surfaces are generally taken to be

$$S_1 = x_1 - x_{1d}, S_2 = x_2 - \alpha_{2f} \quad (6)$$

RBF neural network

The RBF neural network is universal approximator²⁰. It approximates any smooth function $f_n(X): R^n \rightarrow R$.

$$f_n(X) = \theta^T \xi(X) \quad (7)$$

where $X \in D \subset R^n$ is the input vector, $\theta = [\theta'_1, \theta'_2, \dots, \theta'_l]^T \in R^l$ is the weight vector, $l > 1$ is the node number of neuron, and $\xi(X) = [\xi_1(X), \xi_2(X), \dots, \xi_l(X)]^T \in R^l$ is a basic function vector, with $\xi_i(X)$ being chosen as the commonly used Gaussian functions, which have the following form:

$$\xi_i(X) = \exp\left(-\frac{(X - \mu_i)^T (X - \mu_i)}{2\sigma_i^2}\right), i = 1, 2, \dots, l \quad (8)$$

where $\mu_i = [\mu_{i1}, \mu_{i2}, \dots, \mu_{in}]^T$ is the center of the receptive field and σ_i is the width of the Gaussian function.

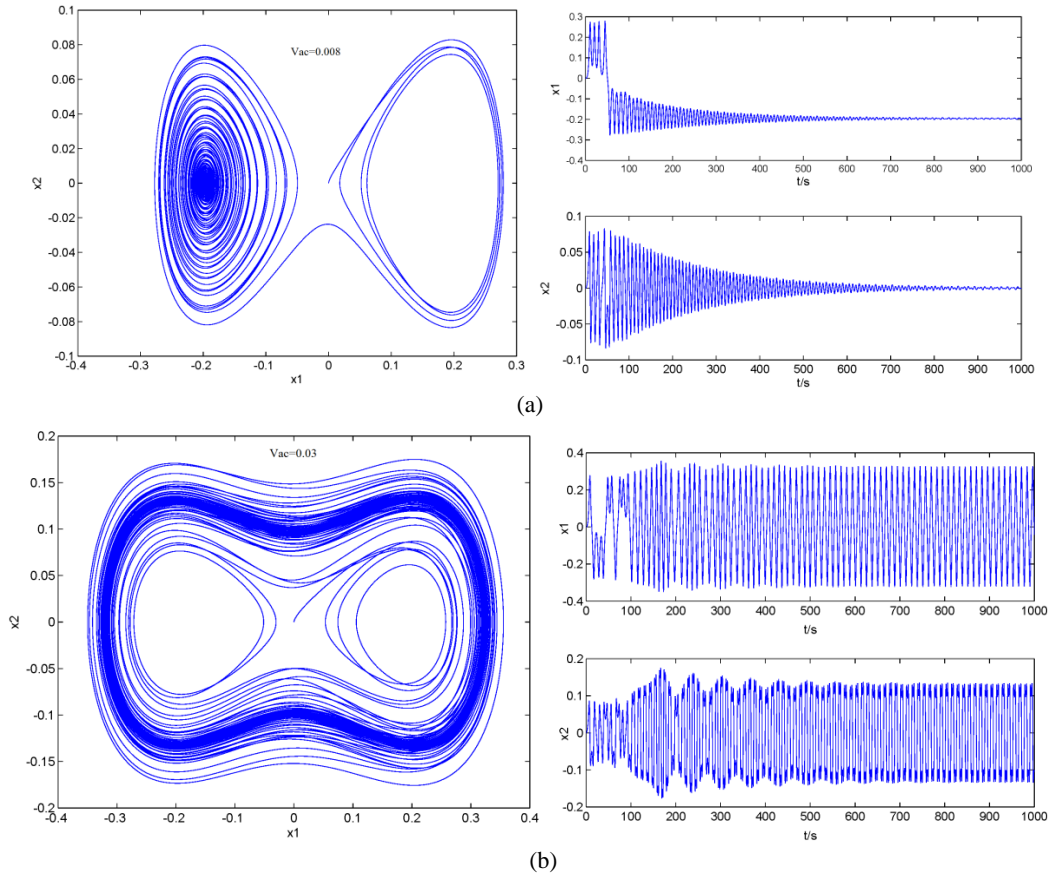


Fig 2.Phase diagrams and corresponding time histories

Due to the approximation capability, the nonlinear term can be approximated as

$$f(X) = \theta^{*T} \xi(X) + \varepsilon \quad (9)$$

where ε is the approximation error, the optimal parameter vector θ^* is bounded and defined as

$$\theta^* = \arg \min_{\theta \in \Omega} \left\{ \sup_{X \in D} |f(X) - \theta^T \xi(X)| \right\} \quad (10)$$

where Ω is the compact region for θ . There exists known constants ε_0 such that $0 < |\varepsilon| \leq \varepsilon_0$.

Controller design

Step 1: Let the Lyapunov function of system be defined as

$$V_1 = \frac{1}{2} S_1^2 \quad (11)$$

Then, taking the time derivative of V_1 along the trajectory (6), it follows that

$$\dot{V}_1 = S_1 (S_2 + y_2 + \alpha_2 - \dot{x}_{1d}) \quad (12)$$

Then, the virtual control input is defined by the following form:

$$\alpha_2 = -k_1 S_1 + \dot{x}_{1d} \quad (13)$$

where k_1 is the design constant.

Substituting (13) into (12), \dot{V}_1 is rewritten as

$$\dot{V}_1 \leq (1 - k_1)S_1^2 + S_1S_2 + \frac{1}{4}y_2^2 \quad (14)$$

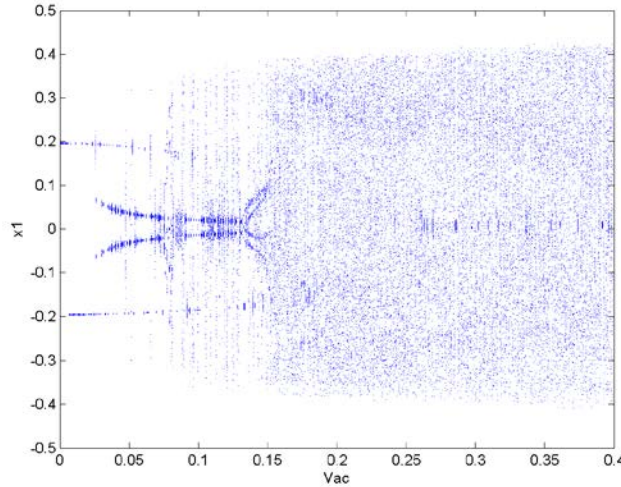


Fig 3.The bifurcation diagram

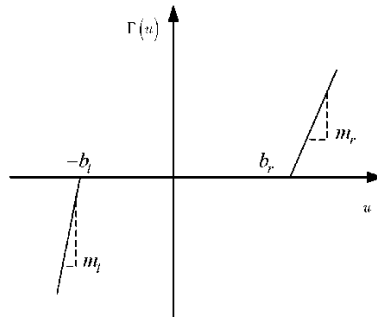


Fig 4. Non-symmetric dead-zone characteristic

Step 2: Filtering α_2 through the first-order filter yields

$$\varpi_2 \dot{\alpha}_{2f} + \alpha_{2f} = \alpha_2, \quad \alpha_{2f}(0) = \alpha_2(0) \quad (15)$$

where ϖ_2 is a time constant.

From (5) and (15), the derivative of α_{2f} is given by

$$\dot{\alpha}_{2f} = -\frac{y_2}{\varpi_2} \quad (16)$$

Then, the derivative of y_2 can be obtained

$$\left| \dot{y}_2 + \frac{y_2}{\varpi_2} \right| \leq B_2(\cdot) \quad (17)$$

According to Young's inequality, there exists

$$y_2 \dot{y}_2 \leq -\frac{y_2^2}{\varpi_2} + y_2^2 + \frac{1}{4} B_2^2 \quad (18)$$

where B_2 is a continuous function.

Introduce the variables as

$$\tilde{\lambda}_2 = \hat{\lambda}_2 - \lambda_2, \tilde{g}_2 = \hat{g}_2 - g_2 \quad (19)$$

where $\hat{\lambda}_2$ and \hat{g}_2 mean the estimation of λ_2 and g_2 .

Choose the Lyapunov function candidate

$$V_2 = V_1 + \frac{1}{2} S_2^2 + \frac{1}{2} y_2^2 + \frac{1}{2\gamma_2} \tilde{\lambda}_2^2 + \frac{1}{2\Gamma_2} \tilde{g}_2^2 \quad (20)$$

where γ_2 and Γ_2 are the design constant of controller.

Then, it is easy to obtain

$$\dot{V}_2 \leq \dot{V}_1 + S_2 (f_2(\cdot) + g_2 u - \dot{a}_{2f}) - \frac{y_2^2}{\varpi_2} + y_2^2 + \frac{1}{4} B_2^2 + \frac{1}{\gamma_2} \tilde{\lambda}_2 \dot{\tilde{\lambda}}_2 + \frac{1}{\Gamma_2} \tilde{g}_2 \dot{\tilde{g}}_2 \quad (21)$$

where $f_2(\cdot) = -\mu x_2 - \alpha x_1 - \beta x_1^3 + G(x_1) + \frac{A}{(1-x_1)^2} \sin(\omega\tau) + d_1$, $g_2 = m$.

In the engineering application, precise measuring for the parameters ($\mu, \alpha, \beta, \gamma, \omega, m, d_1$) of system and actuator dead-zone input becomes difficult because of effect of temperature and material wear, etc. To solve the problem, employ the neural network to approximate the nonlinear coupling function $f_2(\cdot)$.

Therefore, for any given $\varepsilon_2 > 0$, there exists a neural network $\theta_2^{*T} \xi_2$ such that

$$f_2(\cdot) = \theta_2^{*T} \xi_2 + \varepsilon_2 \quad (22)$$

where $\theta_2 = \theta_2^*$.

According to Young's inequality, substituting (14) and (22) into (21) yields

$$\begin{aligned} \dot{V}_2 \leq S_2 \left(\frac{1}{2a_2^2} \lambda_2 S_2 \xi_2^T \xi_2 + g_2 u - \dot{a}_{2f} + S_1 + \frac{1}{2} S_2 \right) - \frac{y_2^2}{\varpi_2} + \frac{5}{4} y_2^2 + \frac{1}{4} B_2^2 + \frac{1}{\gamma_2} \tilde{\lambda}_2 \dot{\tilde{\lambda}}_2 + \frac{1}{\Gamma_2} \tilde{g}_2 \dot{\tilde{g}}_2 \\ + \frac{a_2^2}{2} + (1 - k_1) S_1^2 + \frac{1}{2} \varepsilon_{20}^2 \end{aligned} \quad (23)$$

where a_2 is the design constant.

The actual control law and adaptive laws are given by

$$u = \frac{\hat{g}_2}{\hat{g}_2^2 + \eta_2} \left(-\left(\frac{1}{2} + k_2 \right) S_2 - S_1 - \frac{1}{2a_2^2} \tilde{\lambda}_2 S_2 \xi_2^T \xi_2 + \dot{a}_{2f} \right) \quad (24)$$

$$\dot{\tilde{\lambda}}_2 = \frac{1}{2a_2^2} \gamma_2 \xi_2^T \xi_2 S_2^2 - m_2 \tilde{\lambda}_2 \quad (25)$$

$$\dot{\tilde{g}}_2 = \Gamma_2 (S_2 u - c_2 \tilde{g}_2) \quad (26)$$

where k_2, m_2 and c_2 are the design constant, η_2 is a small positive constant, and $\tilde{\lambda}_2 = \|\hat{\theta}_2\|^2$.

In addition, the inequalities $-\frac{m_2}{\gamma_2} \tilde{\lambda}_2 \dot{\tilde{\lambda}}_2 \leq -\frac{m_2}{2\gamma_2} |\dot{\tilde{\lambda}}_2|^2 + \frac{m_2}{2\gamma_2} |\lambda_2|^2$ and $-c_2 \tilde{g}_2 \dot{\tilde{g}}_2 \leq -\frac{c_2}{2} |\dot{\tilde{g}}_2|^2 + \frac{c_2}{2} |g_2|^2$ are used here.

Therefore, using (24)-(26), it has

$$\begin{aligned}
 \dot{V}_2 &\leq \frac{-\eta_2}{\hat{g}_2^2 + \eta_2} \left(-\left(\frac{1}{2} + k_2\right) S_2 - S_1 - \frac{1}{2a_2^2} \tilde{\lambda}_2 S_2 \xi_2^T \xi_2 + \dot{\alpha}_{2f} \right) S_2 - \frac{1}{2a_2^2} \tilde{\lambda}_2 S_2^2 \xi_2^T \xi_2 - k_2 S_2^2 - \tilde{g}_2 u S_2 - \frac{y_2^2}{\varpi_2} \\
 &\quad + \frac{5}{4} y_2^2 + \frac{1}{4} B_2^2 + \frac{1}{\gamma_2} \tilde{\lambda}_2 \dot{\lambda}_2 + \frac{1}{\Gamma_2} \tilde{g}_2 \dot{g}_2 + (1 - k_1) S_1^2 + \frac{a_2^2}{2} + \frac{1}{2} \varepsilon_{20}^2 \\
 &\leq (1 - k_1) S_1^2 + \left(\frac{1}{2} - k_2\right) S_2^2 + \left(\frac{5}{4} - \frac{1}{\varpi_2}\right) y_2^2 + \frac{1}{4} B_2^2 - \frac{m_2}{2\gamma_2} |\tilde{\lambda}_2|^2 - \frac{c_2}{2} |\tilde{g}_2|^2 + \frac{m_2}{2\gamma_2} |\lambda_2|^2 + \frac{c_2}{2} |g_2|^2 \\
 &\quad + \frac{a_2^2}{2} + \frac{1}{2} (\varepsilon_{20}^2 + \delta_2^2)
 \end{aligned} \tag{27}$$

where δ_2 is the continuous function and satisfies $\frac{-\eta_2}{\hat{g}_2^2 + \eta_2} \left(-S_1 - \left(\frac{1}{2} + k_2\right) S_2 - \frac{1}{2a_2^2} \tilde{\lambda}_2 S_2 \xi_2^T \xi_2 + \dot{\alpha}_{2f} \right) \leq \delta_2(S_1, S_2, y_2, \hat{\theta}_2, \hat{g}_2, x_{1d}, \dot{x}_{1d})$.

In order to illustrate the proposed scheme clearly, the schematic block diagram of the micro-electro-mechanical system with unknown dead-zone input is shown in Fig.5.

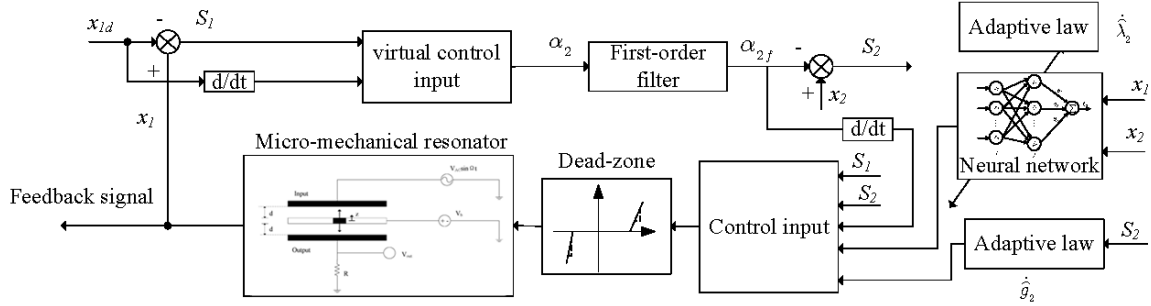


Fig 5. Schematic block diagram of the micro-electro-mechanical system

Stability analysis

Theorem 1: Suppose that chaos controller (24) with updated laws (25) and (26) is used to reduce the trajectory tracking error of the micro-electro-mechanical system with unknown dead-zone input described by (4), by selecting the reasonable parameters as $k_1, k_2, a_2, \gamma_2, m_2, \Gamma_2, \eta_2, \varpi_2, c_2$, then the closed-loop control system is uniformly ultimately bounded, and S_1

converges to a vicinity of zero when the initial condition satisfies $\sum_{i=1}^2 S_i^2 + \frac{1}{\gamma_2} \tilde{\lambda}_2^2 + \frac{1}{\Gamma_1} \tilde{g}_2^2 + y_2^2 \leq 2p$ for any given $p > 0$.

Proof: The derivative of this system with respect to time can be written as

$$\begin{aligned}
 \dot{V} = \dot{V}_2 &\leq (1 - k_1) S_1^2 + \left(\frac{1}{2} - k_2\right) S_2^2 + \left(\frac{5}{4} - \frac{1}{\varpi_2}\right) y_2^2 - \frac{m_2}{2\gamma_2} \tilde{\lambda}_2^2 - \frac{c_2}{2} \tilde{g}_2^2 + b_0 \\
 &\leq -a_0 V + b_0
 \end{aligned} \tag{28}$$

where $b_0 = \frac{1}{4} B_2^2 + \frac{m_2}{2\gamma_2} |\lambda_2|^2 + \frac{c_2}{2} |g_2|^2 + \frac{a_2^2}{2} + \frac{1}{2} (\varepsilon_{20}^2 + \delta_2^2)$, $a_0 > \frac{b_0}{p}$.

Finally, (28) implies that

$$0 \leq V(t) \leq \frac{b_0}{a_0} + \left(V(t_0) - \frac{b_0}{a_0} \right) e^{-a_0(t-t_0)} \leq \frac{b_0}{a_0} + V(t_0) \tag{29}$$

Numerical Simulation

In this section, the numerical simulation demonstrates the effectiveness of the proposed scheme in suppressing the oscillatory and chaos motion of the micro-electro-mechanical system.

The initial conditions are set as $x_1(0) = 0.3, x_2(0) = 0.1$. The given reference signal is given as $x_{1d} = 0.07 \sin(3t) + 0.08 \cos(2t)$. The parameters of the controller are selected as $k_1 = 15, k_2 = 35, \gamma_2 = 0.5, m_2 = 0.3, c_2 = 15, a_2 = 30, \Gamma_2 = 0.04$ and $\eta_2 = 0.001$. The initial values of estimates are set to be $\hat{g}_2(0) = 0.1, \hat{\lambda}_2(0) = 0.3$, and the first-order filter constant is selected as $\varpi_2 = 0.01$. In addition, the RBF neural network are chosen in this way. The center of neural network μ_i is uniformly distributed in the field of $[-5,5]$, and its width σ_i is equal to 2.

The unknown dead-zone input-output characteristic which appears at the sixth second is defined as

$$\Gamma(u) = \begin{cases} 0.9(u + 0.6) & \text{if } u \leq -0.6 \\ 0 & \text{if } -0.6 < u < 0.4 \\ 1.1(u - 0.4) & \text{if } u \geq 0.4 \end{cases}$$

The simulation results of the state response are displayed in Fig.6. Four kinds of curves basically overlap with deadzone on the whole time. Fig.7 shows that the tracking errors between actual signal and desired signal are equal to $\pm 10^{-3}$ for different value of AC voltage. Obviously, the system state x_1 can track the given smooth reference signal x_{1d} precisely.

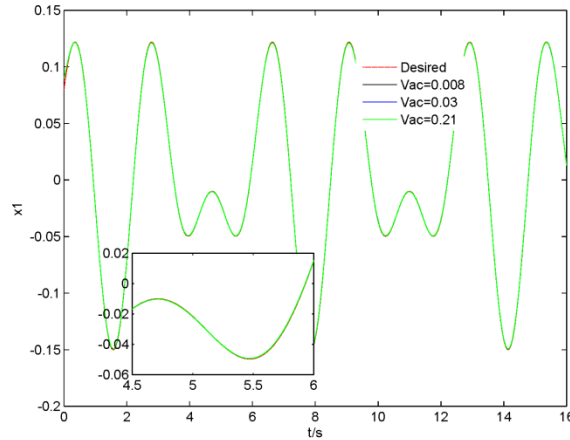


Fig 6. Tracking performance with varying AC voltage

Comparing with phase trajectory in Fig. 2(a-c), the effectiveness and feasibility of the proposed control scheme in suppress the chaos motion can be demonstrated in Fig. 8.

The curves of the actual control are shown in Fig.9. It should be noticed that a key role of designing controller is to try to avoid vibration of control input effectively within the threshold of the non-symmetric dead-zone. This means that the micro-electro- mechanical system possesses excellent tracking performance, and the chattering phenomenon of the controller is greatly weakened.

To further illustrate the changes of the non-symmetric input model parameters which do not influence the performance of the micro-electro-mechanical system, another simulation by changing the model parameters is executed at the sixth second as

$$\Gamma(u) = \begin{cases} 1.1(u + 0.7) & \text{if } u \leq -0.7 \\ 0 & \text{if } -0.7 < u < 0.3 \\ 0.9(u - 0.3) & \text{if } u \geq 0.3 \end{cases}$$

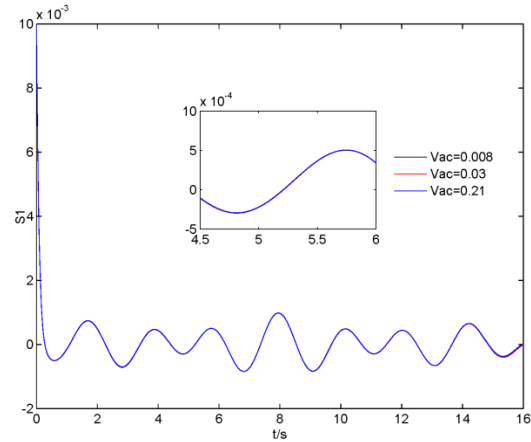


Fig 7. Tracking error with varying AC voltage

The simulation results are shown in Fig.10. Obviously, the closed-loop system still has excellent robustness. It can be known that vibration phenomenon does not appear in the actual control within the threshold of the non-symmetric dead-zone. Additionally, the control input is chatter-free even if the overall system confronts with uncertainty and varying AC voltage.

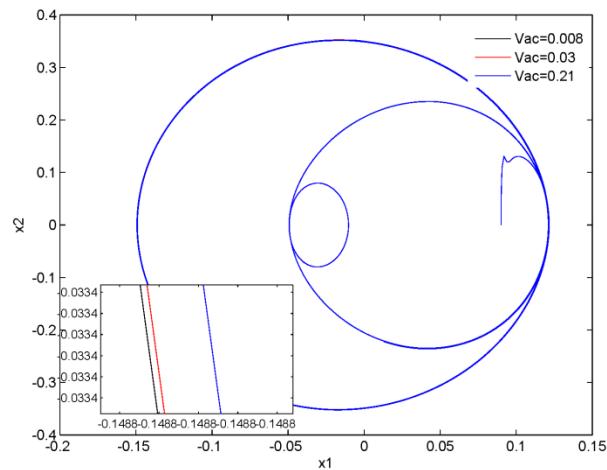


Fig 8. Phase trajectory with varying AC voltage

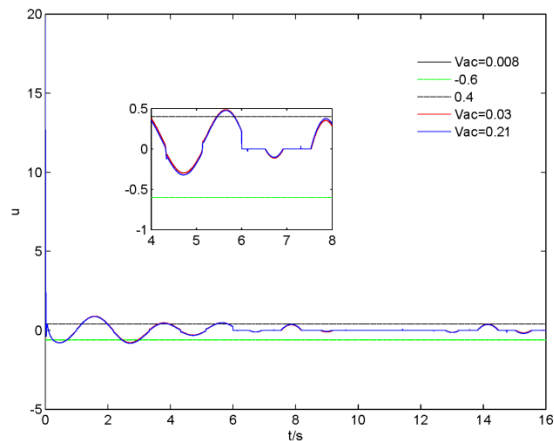


Fig 9. The curve of the actual control with varying AC voltage

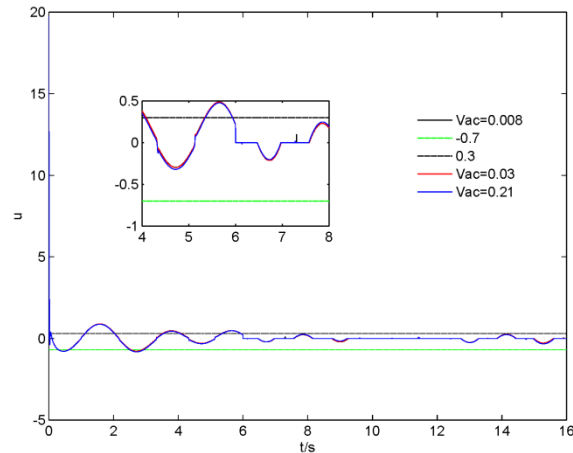


Fig 10. The curve of the actual control with varying AC voltage

Conclusion

This paper discusses adaptive dynamic surface control of chaotic micro-electro-mechanical system because of nonlinear coupling between the electrostatic force and resonator deflection. The transient chaos behavior accompanying with increase of AC voltage can destroy system stability disastrously. An adaptive dynamic surface approach via neural network for eliminating and stabilizing the chaotic motion is developed to oblige system state to approximate a reference signal with small error and compensate parameters variation in the presence of non-symmetric dead-zone input. The presented scheme can guarantee the closed-loop error system is stable in the sense of uniform ultimate boundedness. The more precise parameters of system model and the boundedness hypothesis of control gain which are available in advance in previous works can be cancelled automatically. Finally, numerical simulations for the micro-electro-mechanical system are given to demonstrate the effectiveness of the presented scheme.

Acknowledgments

This work was supported by the National Natural Science Foundation of China (No. 51505170), China Postdoctoral Science Foundation funded project (No. 2015M572445), Chongqing Postdoctoral Science Foundation funded project (No. Xm2015017) and Natural Science Foundation of the Jiangsu Higher Education Institutions of China (No.14KJB460002). The authors also gratefully acknowledge the helpful comments and suggestions of the reviewers and editors, which have greatly improved the presentation.

References

- [1] M. S. Siewe and U. H. Hegazy, "Homoclinic bifurcation and chaos control in MEMS resonators," *Applied Mathematical Modelling*, **35**, 5533–5552 (2011).
- [2] E. M. Miandoab, A. Yousefi-Koma, H. N. Pishkenari, and F. Tajaddodianfar, "Study of nonlinear dynamics and chaos in MEMS/NEMS resonators," *Communications in Nonlinear Science & Numerical Simulation*, **22**, 611–622 (2015).
- [3] J. Sharma and D. Grover, "Thermoelastic vibrations in micro-/nano-scale beam resonators with voids," *Journal of Sound and Vibration*, **330**, 2964–2977 (2011).
- [4] E. M. Miandoab, H. N. Pishkenari, A. Yousefi-Koma, and F. Tajaddodianfar, "Chaos prediction in MEMS-NEMS resonators," *International Journal of Engineering Science*, **82**, 74–83 (2014).
- [5] H. S. Haghghi and A. H. D. Markazi, "Chaos prediction and control in MEMS resonators," *Communications in Nonlinear Science & Numerical Simulation*, **15**, 3091–3099 (2010).
- [6] M. F. Danca, "Random parameter-switching synthesis of a class of hyperbolic attractors," *Chaos*, **18**, 033111 Sep (2008).
- [7] H. Ma, V. Deshmukh, E. Butcher, and V. Averina, "Delayed state feedback and chaos control for time-periodic systems via a symbolic approach," *Communications in Nonlinear Science & Numerical Simulation*, **10**, 479–497 (2005).
- [8] H. T. Yau, C. C. Wang, C. T. Hsieh, and C. C. Cho, "Nonlinear analysis and control of the uncertain micro-electro-mechanical system by using a fuzzy sliding mode control design," *Computers & Mathematics with Applications*, **61**, 1912–1916 (2011).
- [9] M. Roopaei and M. Z. Jahromi, "Synchronization of two different chaotic systems using novel adaptive fuzzy sliding mode control," *Chaos*, **18**, 033133 (2008).
- [10] Bagheri and J. J. Moghaddam, "Simulation and tracking control based on neural-network strategy and sliding-mode control for underwater remotely operated vehicle," *Neurocomputing*, **72**, 1934–1950 (2009).
- [11] S. Zhankui and K. Sun, "Nonlinear and chaos control of a micro-electro-mechanical system by using second-order fast terminal sliding mode control," *Communications in Nonlinear Science & Numerical Simulation*, **18**, 2540–2548 (2013).

- [12] D. Swaroop, J. K. Hedrick, P. P. Yip, and J. C. Gerdes, "Dynamic surface control for a class of nonlinear systems," *IEEE Transactions on Automatic Control*, **45**, 1893-1899 (2000).
- [13] S. I. Han and J. M. Lee, "Adaptive dynamic surface control with sliding mode control and RWNN for robust positioning of a linear motion stage," *Mechatronics*, **22**, 222-238 (2012).
- [14] S. Luo, "Adaptive fuzzy dynamic surface control for the chaotic permanent magnet synchronous motor using Nussbaum gain," *Chaos*, **24**, 5880-5885 (2014).
- [15] Y.-J. Liu and Z.-F. Wang, "Adaptive fuzzy controller design of nonlinear systems with unknown gain sign," *Nonlinear Dynamics*, **58**, 687-695 (2009).
- [16] S. Ibrir and C.-Y. Su, "Simultaneous state and dead-zone parameter estimation for a class of bounded-state nonlinear systems," *IEEE Transactions on Control Systems Technology*, **19**, 911 - 919 (2011).
- [17] D. J. Li, "Neural network control for a class of continuous stirred tank reactor process with dead-zone input," *Neurocomputing*, **131**, 453-459 (2014).
- [18] P. J and D. R, "Identification and adaptive neural network control of a DC motor system with dead-zone characteristics," *ISA Transactions*, **50**, 588-598 (2011).
- [19] X. Wu, X. Wu, X. Luo, Q. Zhu, and X. Guan, "Neural network-based adaptive tracking control for nonlinearly parameterized systems with unknown input nonlinearities," *Neurocomputing*, **82**, 127-142 (2012).
- [20] R. J. Wai, J. X. Yao, and J. D. Lee, "Backstepping fuzzy-neural-network control design for hybrid maglev transportation system," *IEEE Transactions on Neural Networks & Learning Systems*, **26**, 302-317 (2015).